High Speed Deterministic Polishing of Strongly Aspherical Mirrors

ESA Contract No 4000114781/15/NL/PS/gp

Executive Summary Report

ESR

Doc. nr :	2249-01-08
Issue :	1
Date :	07/09/2020

	NAME	DATE	SIGNATURE
Prepared by	V. MOREAU	07/09/2020	
Checked by	C. FLEBUS	07/09/2020	
Released by	V. MOREAU	07/09/2020	

DISTRIBUTION LIST

Name	Company	Quantity
Configuration Office	AMOS	1 copy
Vincent MOREAU	AMOS	1 soft copy
Luca MARESI	ESTEC	1 soft copy
Roman WINDPASSINGER	ESTEC	1 soft copy

CHANGE RECORD

ISSUE	DATE	NB OF PAGES	MODIFIED PAGES	REMARKS
1	07/09/2020	22	All	Initial Issue

TABLE OF CONTENTS

List of Acronyms and Abbreviations

The list of Acronyms and Abbreviations used in this document is given hereunder:

CCP	Computer Control Polishing
CGH	Computer Generated Hologram
CMM	Coordinate Measuring Machine
CTE	Coefficient of Thermal Expansion
FEM	Finite Element Model
FJP	Fluid Jet Polishing
FoM	Figures of merits
FoV	Field of View
IBF	Ion Beam Figuring
LR	Low Roughness mirror
LW	Lightweighted Mirror
MRF	Magneto Rheological Finishing
NIR	Near Infra-Red
P-V	peak to valley
RMS	Root Mean Square
SFE	Surface Form Error
SiC	Silicon Carbide
SPDT	Single Point Diamond Turning
SSI	Sub aperture Stitching Interferometry
TVAC	Thermal Vacuum
UV	Ultra-Violet
VIS	Visible
WFE	Wavefront Error

1. INTRODUCTION AND STATE-OF-THE-ART

Fast, off-axis, highly aspheric or even free form reflective designs have lately been increasingly investigated and studied in order to build compact, lightweighted and high performances space-based instruments.

In the UV-VIS wavelength ranges, the roughness and surface accuracy requirements of the optics are usually much more stringent than in NIR-IR. Indeed, scattering increases rapidly at shorter wavelengths also the impact of mirror surface error is proportional to the light frequency.

Recent advances in melt-spinning technology, novel aluminum alloys development and metallic mirrors manufacturing open up new perspectives for full-metallic instruments with challenging design such as compact spectrometers, large FoV telescopes or relay systems, to be used -or tested – at ambient temperature and/or at cryogenic conditions.

The HiDeAs project aims to demonstrate that metallic mirror manufacturing processes can be controlled in a deterministic way, so that the production of UV-VIS highly aspherical optics can be achieved in a limited number of iterations, for a controlled cost and in well-defined timetable.

Another key objective of the project is to demonstrate that the a-thermal properties of a full-aluminum (or full-metallic) instrument design can be maintained over a large thermal range and especially at very low temperatures (e.g. < 200K). In this purpose the limitations imposed by the bi-metallic effect and thermal stresses due to different CTE (e.g. substrate and plating) are particularly important.

Finally, the mechanical design of the produced mirrors shall be finely optimized in order to satisfy both constraints of low areal density and high stiffness.

The demonstration of technologies and processes has been carried out by the manufacturing and testing of two strongly aspherical mirrors:

- One with the specifications of a lightweighted primary mirror of an aspherical telescope. This mirror is referred as ***Lightweighted mirror*** (LW mirror) in the following of this document.
- The other suitable for an element of a spectrometer requiring very low roughness and operating at temperature of 200K. This mirror is referred as ***Low Roughness mirror*** (LR mirror) in the following of this document.

These specifications and mirrors design have been established in order to fulfil the performances of two specific instruments:

- The LW mirror is the primary mirror of the ProbaV EVO Three Mirror Anastigmatic telescope developed by OIP in the frame of ESA GSTP 4000115882/15/NL/GLC/fk
- The LR mirror is the Tertiary mirror of a high resolution imaging spectrometer based on a holographic free form grating (CHIMA), designed and prototyped by AMOS under ESA contract 4000117881/16/NL/PS.

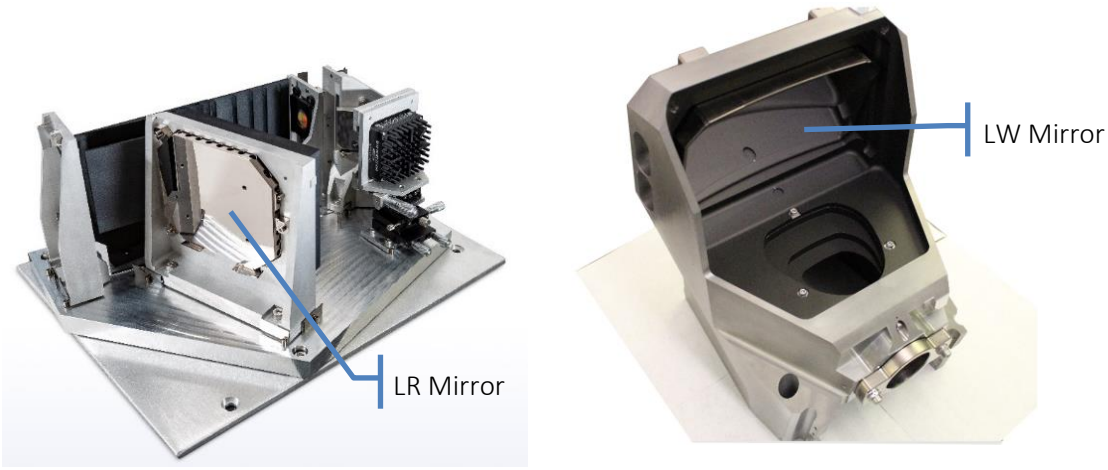

Figure 1 : Left – CHIMA spectrometer including LR mirror (back-face view). Right – LW mirror integrated in PV-EVO Telescope (front face view)

1.1 SUBSTRATE MATERIAL FOR SPACE LIGHTWEIGHTED MIRRORS

Mirror materials must be selected regarding the specifications, the environmental constraints and the performance required for a specific mission, as well as the manufacturability. Based on the experience of Amos, a few materials have been preselected and compared with respect to the most common figure of merits.

Material selection	Figure of merit
• Al6061 (Rapid Solidified Aluminum) • AlSi40 + NiP (Aluminum Silicon Alloy + Nickel plating) • Be + NiP (Beryllium + Nickel plating) • SiC (Silicon Carbide) • ZERODUR (Ultra Low CTE Glass)	• The Specific stiffness The ratio of the elastic modulus over density, because lighter and stronger material answer better to vibration and mechanical constraints in embedded systems. • The Thermal stability The ratio of the conductivity over the CTE, because a fast stabilization of a gradient of temperature and a low impact of the temperature on mechanical distortion is preferable for an environment where temperature can vary fast like in orbit or in space. • The Ultimate tensile strength The Maximum stress that the material can withstand before breaking. • The manufacturability (including cost, time, quality and environment)

A comparison of the specific stiffness and thermal stability between is shown on Figure 2.

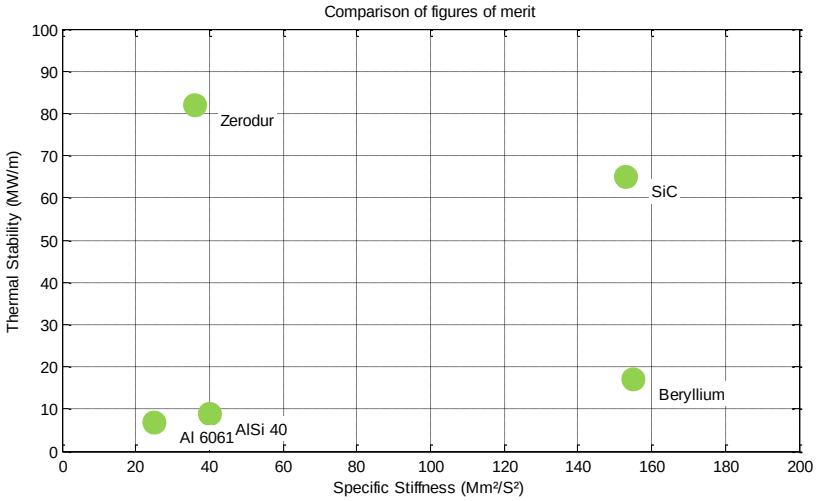

Figure 2, comparison of the Thermal stability with Specific stiffness. Higher values are better. SiC is the most versatile material with relatively high values for both FoM. AlSi has significantly better specific stiffness than 6061 grade.

Within the HiDeAs project, AMOS has developed a methodology to compare the structural performances of materials, by considering not only the intrinsic characteristics, but also the lightweighting design adapted to each material, considering the polishing pressure and design limit stress. The outcome of this approach is summarized by the following graph that define, for each material, the optimum parameters for lightweighting structure.

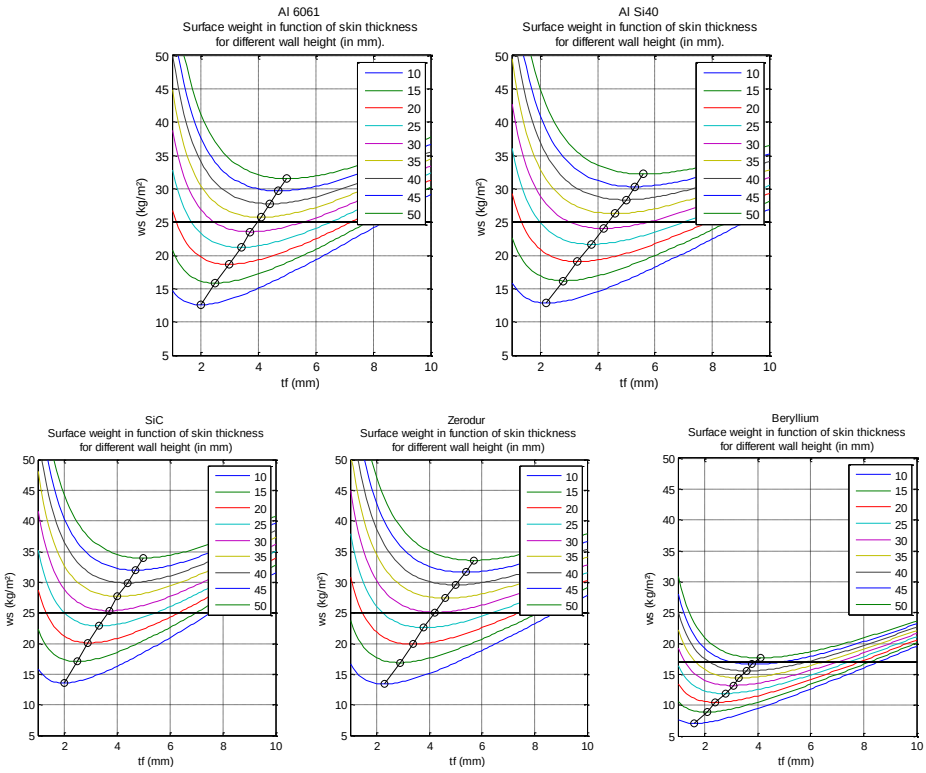

Figure 3 : set of curves to determine the optimal skin thickness and pockets height for a given areal weight objective. For low skin thickness, the weight of the structure is comparable to the weight of a structure having a high number of small cells. For large skin thickness, the weight is comparable to the weight of a solid mirror. Between these 2 extreme configurations, there is a skin thickness giving an optimal structural design. The optimal points are given by the dots on the black line joining the minimums of each curves.

The value of the cell size (inscribed diameter of triangular back pockets) is calculated to guarantee that the quilting of the surface, generated by the polishing pressure, is not higher than a predefine limit. In the study we chose a quilting of $\delta \approx 8$ nm. As the polishing pressure and optimal skin thickness differ for all material, all the cell sizes are different.

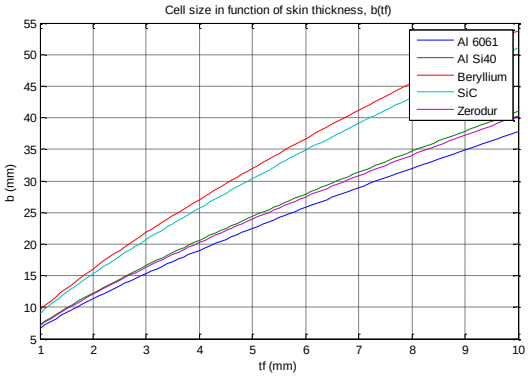

Figure 4, calculated curve showing the relation between cell size and skin thickness in order to guarantee quilting effect < 8 nm PtV.

The conclusion of our material study is that, on larger mirrors (typ. >300 mm diameter), Silicon Carbide and Beryllium offer advantages over Aluminum and glass, including higher specific stiffness and fracture toughness (compared to Zerodur).

For smaller mirrors (typ. <300mm diameter), these advantages are less significant because good flexural performances can be achieved for low areal density in all materials. For this class of mirrors, plated aluminum alloys offer the advantage of low cost, and processing facility which enables the use of very efficient machining technics such as Single Point Diamond Turning of optical surface and interfaces. With respect to ceramics (SiC and Zerodur) aluminums also offer a higher design limit stress, and then a better guarantee against launch and shock constraints.

It must be noted that structural properties alone cannot always dominate the choice of material. The difference in thermal properties can also be significant for missions with rapidly varying radiative loads. In such a case low expansion glass are definitely superior to aluminum, but SiC is once again offering the best compromise, with an almost equivalent thermal stability and largely better specific stiffness.

1.2 DETERMINISTIC MANUFACTURING AND POLISHING TECHNICS

The choice of polishing and figuring technics depends on the type of defect to improve, roughness or shape, the type of material and the manufacturing limitation. The convergence rate is a good indicator of the determinism of the process. It is given by the ratio between achieved surface correction (in nm rms) and goal surface correction (in nm rms). With a good convergence rate (typically > 70%), it is possible to predict in advance the number of iteration necessary for a given surface. However, the determinism is affected by other factors than the convergence rate. A figuring method can degrade the roughness obtained in a previous step, making necessary to reiterate other steps.

The most accurate polishing and figuring technics to date are summarized here below :

- Single Point Diamond Turning (SPDT) is a precision machining process using a single crystal to cut metal substrate. It is a convenient method to produce off-axis, strongly aspherical and freeform mirrors. Because the tool displacement is controlled with precision, it is possible to manufacture, in one go,

alignment references and optical surface with great precision, reducing the efforts for alignment at a further stage. Defects of different nature are expected at the end of the run: the tool will always leave periodical grooves at the surface, so a roughness of about 10 nm P-V on aluminum is ultimately achieve. For better roughness, SPDT shall be used in combination with complementary methods as Computer Controlled Polishing.

- Computer Control Polishing (CCP) could be seen as an automatization of manual polishing technics. The polishing tool uses a slurry with abrasive grains and a friction pad coupled with a cardan joint to move the pad parallel to the surface. From an initial measurement of surface errors, one determine the dwell function (or dwell time) that gives the necessary polishing time at specific location to correct the errors. CCP is ideal to improve the roughness of surface, the inconvenient is that the size of the pad cannot be infinitely small, causing that shape variation of small size cannot be corrected. This makes CCP more adapted for large spherical or slightly aspherical mirror than for strongly aspherical mirror. As an alternative to rigid polishing pads, Bonnet polishing uses a rotating inflated spherical membrane tool (the "bonnet"), which naturally molds itself to the local aspheric surface and maintains stability to provide natural smoothing.

- Magneto Rheological Finishing (MRF) is also a mechanical, but non-contact, polishing process. A slurry is applied on a wheel (or ribbon) and the wheel is rotating on top of the surface to polish. The slurry contains abrasive grains suspended in a magnetorheological fluid. When a magnetic field is applied near the fluid, the ferrous particles align with the magnetic field lines and push the abrasive toward the surface. This process has a relatively low removal rate but a good figure of convergence > 85% on most common materials. MRF can be used to improve figure and roughness of diamond turned optics However, some frequencies (grooves of 50-500µm width) are difficult to remove. Most of the MRF machine integrates a performant interferometer to measure the mirror without removing it from the machine.
- Fluid Jet Polishing (FJP) use a pipe that delivers a jet of abrasive slurry to graze the surface. Like for the CCP and MRF, the dwell time is calculated from the measurement of the erosion function and the error map. A good convergence rate, up to 80%, was already demonstrated with this technic that can be applied to all material. This method does not suffer from edge effects as the pressure depend only on the fluid dynamics and the location of the pipe.
- Ion Beam Figuring (IBF) is a non-contact method in which the removal of material is caused by sputtering of ions, generally argon, onto the surface. Ions from a plasma are accelerated and hit the surface with a sufficient momentum to remove material. The operation occurs in a vacuum chamber with a pressure below 10^{-4} mbar. The erosion rate is slow and it requires a minimum of pre-polishing. As the erosion is predictable, it gives a deterministic method with convergence up to 90%. It is also insensitive to the edge effect that are typical to mechanical polishing tools. Unfortunately, this process can amplify digs and scratches and reveal sub-surface damage, for that raison it is commonly used in combination with mechanical polishing technics.

1.3 TECHNOLOGIES FOR TESTING ASPHERICAL MIRRORS

Without accurate measurements, it would not be possible to manufacture quality mirror. Different metrological devices are used during the figuring or polishing of mirrors. At each step of the process, the surface is inspected to find deviations and determine the necessary iteration. An accurate and online measurement is ideal to converge towards the desired surface. The time and cost of the operation are also important to select the appropriate testing instrument. We describe here different metrology principles and their usage at different stage of the production :

- Interferometric technics : A figure of interference, called interferogram, is created by difference in optical path between a coherent beam reflected by the object surface and the beam reflected by a reference surface. In a null testing configuration, this reference surface is the ideal surface. In this case, the interferogram shows directly the deviation (= the height difference between the measured and the ideal surface). Null testing requires compensation optics to shape the beam of the ideal surface. For Aspherical surfaces one suitable compensation optic is the Computer Generated Hologram or CGH. Unfortunately, CGH is expensive and limited to a specific surface shape. Other problems are that basic interferometers are sensitive to vibrations and inhomogeneity in pressure and temperature.

- Deflectometry : A deflectometer determines the slopes of a surface by measuring the reflection angles of light rays. The slopes need to be integrated to calculate the surface height. Practically, the tested surface reflects a periodic grid generated by a spatially light modulator (SLM) towards a camera. The local slope of the surface is detected as a local phase shift of the periodic image on the camera. Deflectometry is more sensitive to high spatial frequency than low spatial frequency. Therefore, the height sensitivity can be limited to a few µm for a deformation with the size of the total aperture. The advantages compare with the interferometer, is that it is not based on the light interference and does not suffer of sensitivity to noises and vibrations.

- Non-contact profilometry : these methods are generally based on the sensing of an optical beam scanning the tested surface. An example of optical profilometer is the Luphos sensor, based on Multi Wavelength Interferometry. The technology use 4 independent wavelengths to provide measurements with nanometric accuracy. The beating frequency of the 4 wavelengths is used to measure an absolute distance and extend the measurement range to 1.25 mm, greater in comparison to the range of single wavelength interferometry. During the measurement, the object rotates on its stage and the probe is translated to record a spiral scan of the whole surface.

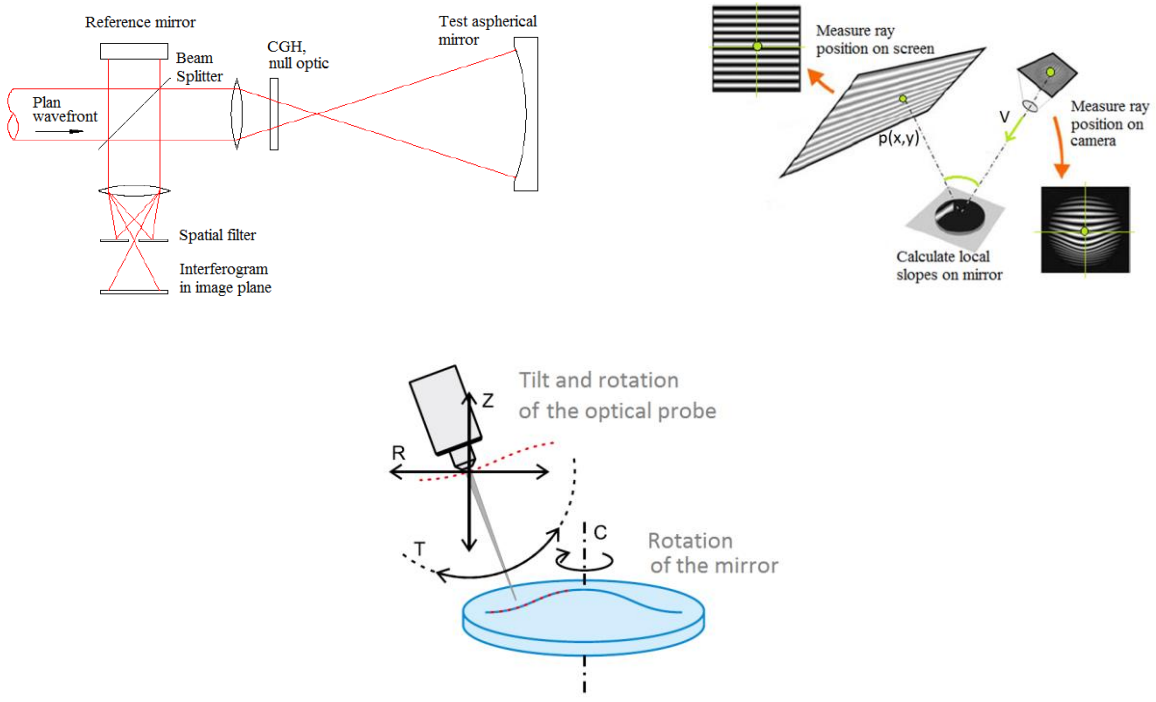

Figure 5 : Left - null test of an aspherical mirror using a CGH. Right - principle to measure the slopes on a surface with deflectometry. Bottom – Non-contact profilometry with an optical probe.

1.4 SELECTIONS OF MATERIAL, PROCESS AND METROLOGY FOR HIDEAS STUDY

We showed that the determinism of a manufacturing process is affected by the convergence rate but also by the nature and shape of the polishing tool and the stability of the erosion. We explained that the range limitation of the metrology system and the ability to integrate them in a manufacturing process have an impact on the manufacturing time.

For this project, **Single Point Diamond Turning of Nickel plated AlSi alloy** has been selected because of:

- The ability of SPDT manufacturing process to generate Strong Aspheric surface shape within an initial accuracy of < 50 nm rms SFE and <0.1 mm RoC error, so directly in the range of applicability of highly deterministic figuring technics such as Ion-beam, Fluid Jet or Magneto-Rheology figuring.
- The capability of SPDT for maintaining a very accurate referencing of mirror interfaces with respect to Mirror optical axis orientation and vertex location, so that assembly and alignment operation are significantly simplified.
- The homogeneity and machinability of amorphous NiP plating that guaranty an initial surface roughness of < 4 nm rms, so that soft mechanical post-polishing, is expected to be sufficient for achieving < 1 nm rms roughness.
- The possibility of adjusting the CTE of AlSi alloy to a value very close to NiP plating, so that the bi-metallic effect can be minimized over a large temperature range (down to -200K).
- The low cost
- The experience of AMOS in metallic mirror manufacturing.

The selected figuring approach is the **Ion Beam Figuring**, because of its high convergence rate on Nickel plating.

To our knowledge, only **interferometry in combination with Computer Generated Hologram (CGH)** can achieve <10 nm rms surface accuracy on asphere and free form geometries. This is therefore the baseline for the project.

Nevertheless, and in order to further explore the capabilities of more flexible methods, AMOS have also compared the CGH test results with Optical probe and deflectometry approaches that could, later, be implemented in-situ, i.e. on the diamond turning machine axis. The goal is to take advantage of the extremely high accuracy of the lathe axes for positioning of the probe or for referencing the sub-pupils.

2. MIRRORS MANUFACTURING PROCESS AND RESULTS

The manufacturing process is identical for both LW and LR mirrors. The number of figuring iterations is a critical aspect of the project, we initially expect that the LR mirror will request more runs due to the more stringent requirements on surface quality and roughness for LR mirror (5 nm RMS SFE).

The requested mirrors accuracy imposes several precautions such as strict thermal regulation, well stabilised material and high-quality diamond tools.

The complete overview of the workflow is provided in Figure 6.

In order to assess the deterministic control of the process, we report in this section the achieved surface quality, after Single Point Diamond Turning, after post-polishing and during the figuring iteration runs.

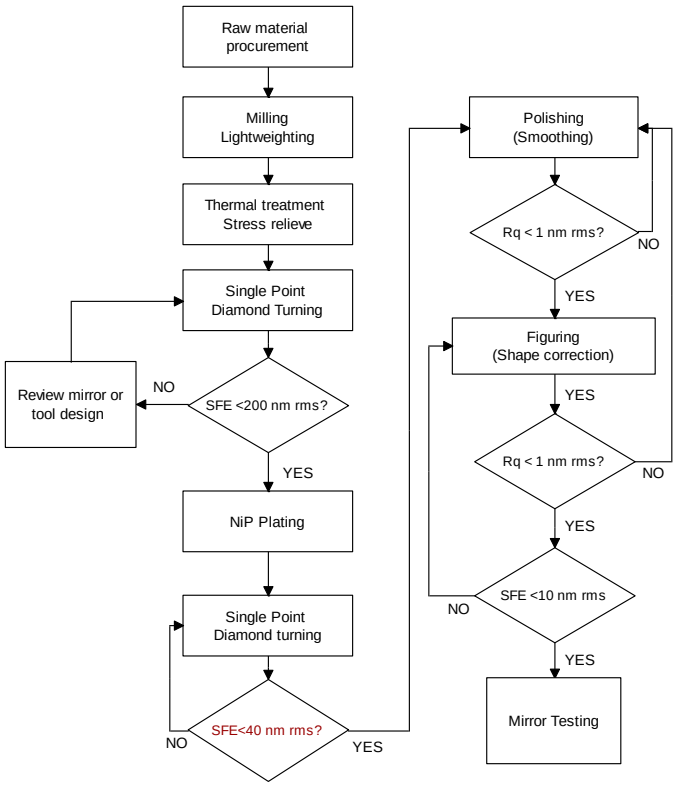

Figure 6 : Workflow for the manufacturing of the LW mirror (similar for the LR mirror)

2.1 SINGLE POINT DIAMOND TURNING

The mirrors have been machined on an ultraprecision lathe Moore 350FG. The axis straightness of this machine is better than 0.2µm on 300mm. Specific tooling were machined at AMOS to clamp the part. The machine is enclosed in a thermal regulated room with a temperature stability < 0.1°C.

All mechanical interfaces of the mirrors were machined to accurately clamp the parts and to avoid any deformations.

The diamond machining has been performed before and after Nickel plating.

After the SPDT operation, the surface error is controlled by interferometry. The mirror SFE is not yet critical at this stage but the objective is to achieve a SFE lower than 40 nm rms, which ensure that the operation is absolutely under control.

On the LW mirror, the achieved surface accuracy after SPDT is 31 nm RMS.

On the LR mirror, the achieved surface accuracy after SPDT is 32 nm RMS.

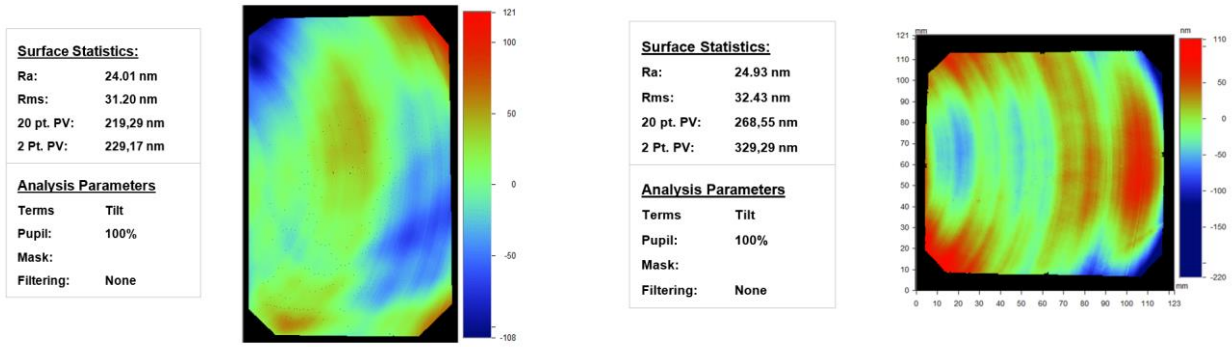

Figure 7 : Right - SFE of LW mirror after Nickel plating and SPDT. Left - SFE of LR mirror after Nickel plating and SPDT

2.2 POST-POLISHING

In order to achieve the demanding required roughness level on the optical surface (Rq roughness <1 nm RMS on LW mirror; Rq roughness <0.5 nm RMS on LW mirror), mechanical post-polishing shall be performed on a 5-axis robot. The post-polishing, due to the low pressure applied by tools, modify the mirror shape, which shall be corrected by Ion Beam Figuring. The achieved roughness is regularly controlled by white light interferometry (ZYGO) over spatial frequencies ranging from 0.6 mm^{-1} to 1500mm^{-1}. The post-polishing process is continued until the required roughness is reached or until no more improvement can be achieved.

During the project, we have faced an unexpected reaction of the nickel plating with the polishing slurry, causing a corrosion reaction over the surface of the LW mirror. This reaction could finally be attributed to a slightly excessive concentration of the Phosphorus content within the NiP layer. It only occurs on this batch of plated mirrors and was not reported again since it has been notified to the sub-contractor.

The corrosion layer has been fixed and removed after a deeper polishing with a stiffer pad. Nevertheless, the surface errors as measure after post-polishing was significantly larger than we would have wanted.

On the LR mirror, plated later in the project and not impacted by corrosion issue, the post-polishing had a quite moderate impact on the surface accuracy.

On the LW mirror, the achieved surface accuracy after post-polishing is 489 nm RMS.

On the LR mirror, the achieved surface accuracy after post-polishing is 47.9 nm RMS.

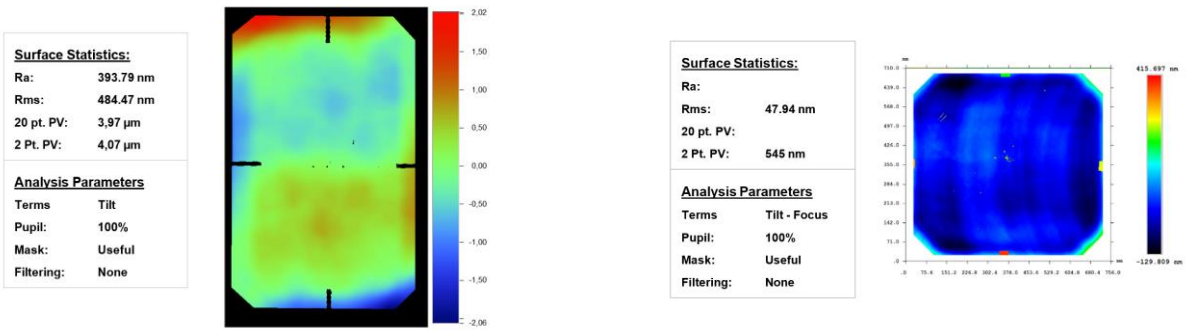

Figure 8 : SFE of LW mirror after Post-polishing

2.3 ROUGHNESS METROLOGY

The roughness of LW and LR mirror has been measured after post-polishing and at the end of the manufacturing process. Roughness have been measured in 5x and x25 magnification

- x5 covers spatial frequencies from 0.6 mm^{-1} to 300 mm^{-1}
- x25 covers spatial frequencies from 3 mm^{-1} to 1500 mm^{-1}

The table below provides typical results (medium results over the different sampled points) achieved for both magnifications.

	X5	X25
LW mirror	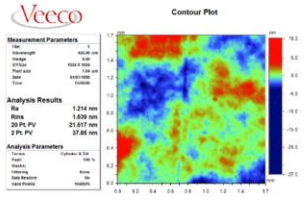 Rq=1.539 nm RMS	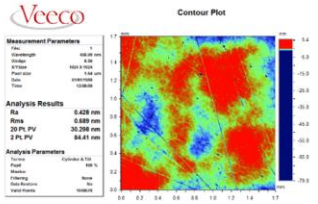 Rq = 0.689 nm RMS
LR Mirror	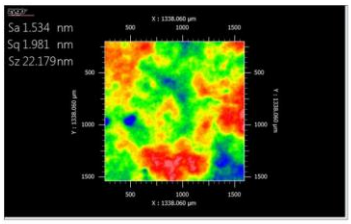 Rq=1.98 nm RMS	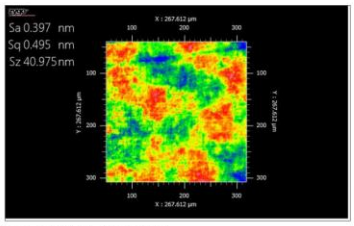 Rq = 0.495 nm RMS

Figure 9 : Achieved Surface roughness for both LW and LR mirror, in x5 and x25 magnification

These results show that the roughness performances are excellent for high frequencies, with residual roughness < 1nm on the LW mirror and <0.5 nm on the LR mirror in x25 magnification. Nevertheless, the applied polishing process, whose objective is mainly to smooth out the high frequency machining grooves, was not as performant for the low frequencies (0.6 to 3 mm^{-1}).

2.4 ION BEAM FIGURING

In order to meet the challenging SFE accuracy for both mirrors, Ion Beam Figuring (IBF) runs have been performed. This process, routinely used at AMOS on materials like SiC, glass, NiP, metals etc., is carried out in the vacuum chamber facility at our premises.

For the HiDeAs project, we specified the following figuring objectives :

- For the LW mirror, the requirement is 10 nm RMS SFE over 80mm diameter sub-pupils, and a maximum of 3 iterations are allowed as a requirement for validation of the determinism of the process.
- For the LR mirror, the requirement is 5 nm RMS SFE over 60 mm diameter sub-pupils. 6 iterations are allowed given the much more challenging SFE objective.

2.4.1 LW mirror figuring

When we look in details the convergency results (Figure 10), we observe a reasonably good convergency (70% to 80%) for the two first IBF runs. Considering the poor initial SFE after post-polishing, these first IBF runs allows a recovery of the surface shape, equivalent to the value achieved by SPDT. Nevertheless, the following runs #3 and #4 did not provide a very significant improvement and the efficiency of the process surprisingly drop to about 20%.

The required performance (21 nm RMS) is well achieved after the Run#4 but we fail in achieving this value in 3 iterations on the mirror due to the poor starting point after post-polishing.

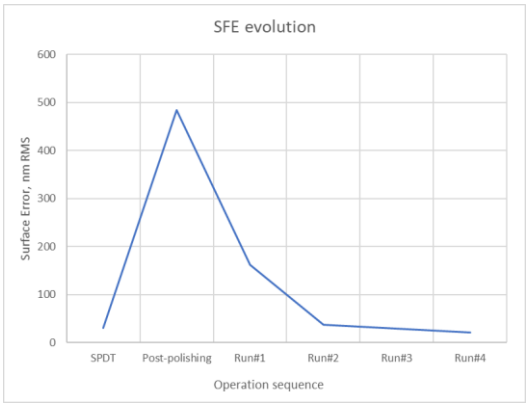

Figure 10 : Evolution of the Surface Form error, from SPDT to the last IBF run.

A finer analysis reveals that the main contribution to the residual surface error is indeed a low frequency component (mainly Coma). This is even more surprising that such low frequency is normally very well corrected by the IBF process. **This led us to conclude that the Coma error is resulting from a deformation of the mirror itself during the IBF process**, which was not observed on other material such as glass of silicon carbide.

A rational hypothesis is that the global heating of the mirror, caused by the transfer of ions energy into the material, is responsible for a further stress release into the blank, resulting in slight deformation that compromise the good convergency of the process.

During the second phase of the HiDeAs project, we have developed a specific thermal treatment for AlSi40 mirror blanks, in order to provide optimal thermal behaviour and long-term stability to this material. This new relaxation process has been validated on a spare LW mirror.

On this spare mirror, the surface error has been achieved after a single run, and definitely meets the sub-pupil requirement of HiDeAs, with a worst case of 9.3 nm RMS and a mean value of 7.17 nm RMS.

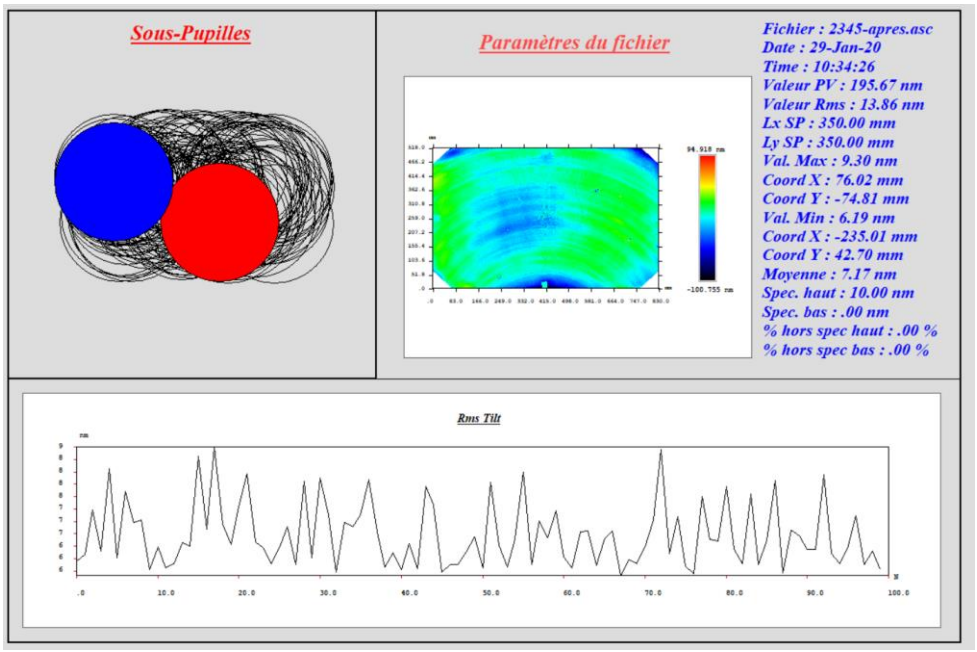

Compliant sub-pupils Monte-Carlo analyses of the Spare LW mirror: Max = 9.3 nm RMS, Mean = 7.2 nm RMS

2.4.2 LR mirror figuring

Due to a much better starting point after post-polishing, only 2 iterations were finally sufficient for achieving the required surface quality on the LR mirror. The converge rate is about 70% for the first iteration and remains stable for the second one.
The Monte-Carlo analyses performed on the sub-pupil concludes that 80% of the sub-pupils are compliant with the requirement of SFE < 5 nm rms, the remaining 20% are below 6.4 nm rms.

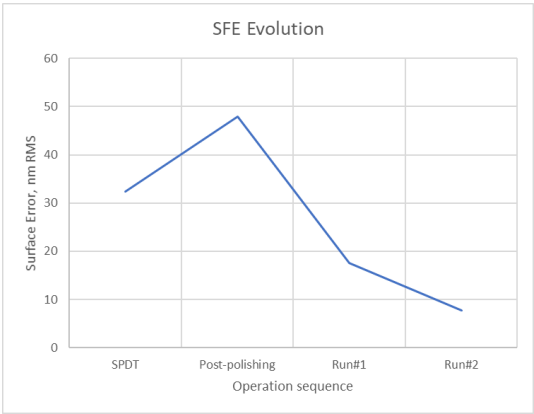

Figure 11 : Evolution of the Surface Form error, from SPDT to the last IBF run.

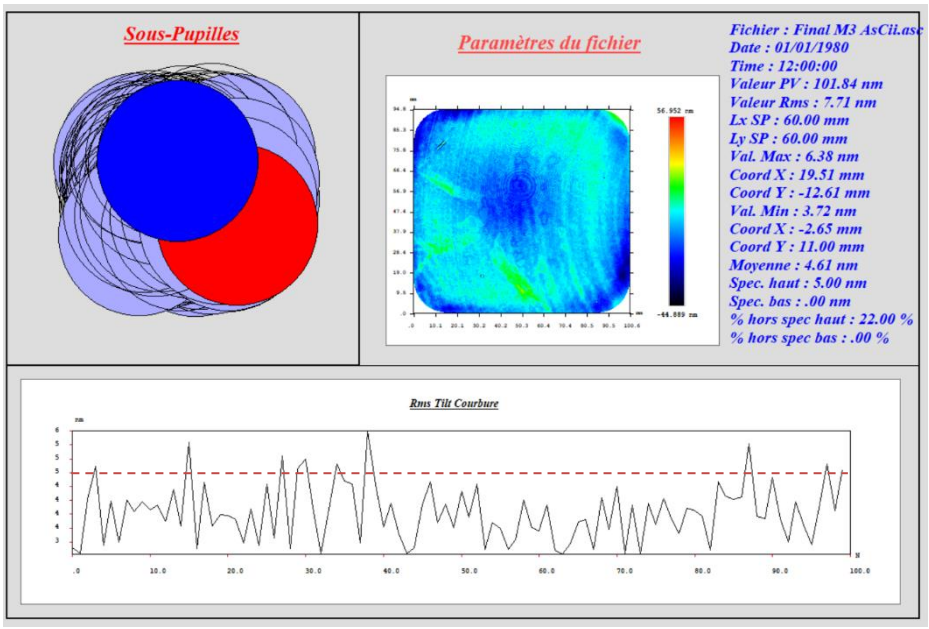

Figure 12 : Monte-Carlo analyses of 60 mm diameter sub-pupils over the useful area. Mean value is 4.61 nm rms with about 80% of the sub-pupils below 5 nm rms. Worst sub-pupil is 6.38 nm rms.

3. IN-SITU METROLOGY

A side objective of the project was to implement an alternative method for the in-situ metrology of optical surfaces.

The benefits of such approach are multiple:

- To provide accurate data for a quick correction of repeatable errors in a second iteration of SPDT.
- To objectify the performance of lower cost and universal alternative method (compared to CGH) for measuring highly aspherical or freeform mirrors.
- To determine the cases (relaxed requirement, type of surface, type of errors) where these metrologies could be competitive to CGH.

In accordance with the conclusion of the State-of-the-art study, the deflectometry method have been identified as offering the best potential. A tests campaign has been conducted with the Belgian company Lambda-X who commercialize this technology for ocular lenses, and who is our partner on this project.

In summary, the feasibility of using a deflectometer device for in situ measurement of mirrors on a lathe has been validated successfully. The high accuracy of the lathes' axes allowed a precise calibration of the apparatus in terms of mirror slopes, and the resolution of the system was found to be 12 µrad.

A rectangular (Cartesian) scan were performed on a highly freeform mirror to validate the feasibility of this method. We demonstrated the detection of 100 nm PtV waviness defects that have been confirmed by interferometry.
The results of this measurement campaign have already been used in the design of the next iteration of the instrument, supported by a new GSTP project (GSTP El. 2 AO7935 "MICA: Optical characterization of high-precision mirror").

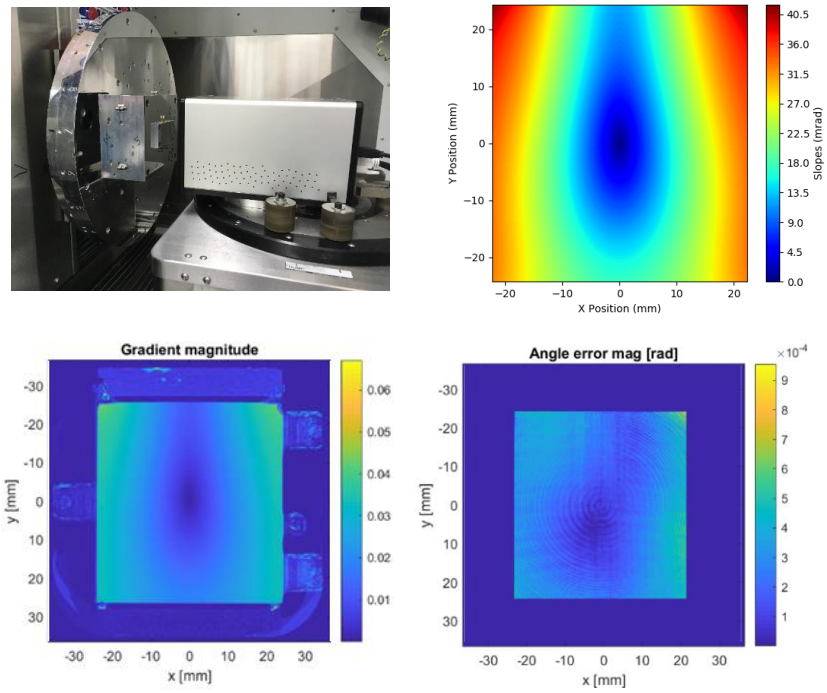

Figure 13 : Top left – Implementation of the NIMO deflectometer in the diamond turning lathe. Top right – theoretical surface slope (as designed). Bottom left - Slopes measured with the deflectometer. Bottom right - Slope errors with respect to theoretical surface slope.

4. THERMAL STABILITY PERFORMANCE

The thermal stability of Aluminum mirrors is a major concern for application in space. In a 2014 paper*, Fraunhofer Institute for Applied Optics reports stability tests within the AlSi40 alloy plated with NiP. The authors show that the dimensional stability of AlSi composites is a challenge due to thermal mismatch stresses of the two phases, aluminum and silicon.

In the frame of the HiDeAs project, we have performed several tests to demonstrate and ultimately secure a thermal stabilization process inspired, but not exactly identical, to the one proposed by IOF.

4.1 LIGHTWEIGHTED MIRROR THERMAL AND LONG-TERM STABILITY

We report here the results of this thermal stability test, performed on the Spare LW mirror.

* J. Kinast, K. Grabowsky, A. Gebhardt, R-R Rohloff, S. Risse, A Tünnermann, "Dimensional Stability of Metal Optics on Nickel Plated AlSi40", Proc. SPIE 10563, International Conference on Space Optics — ICSO 2014, 105635W

The initial surface shape is presented in Figure 14, the surface of the AlSi40 blank is just diamond turned, no NiP layer is applied at this stage.

Interferogram

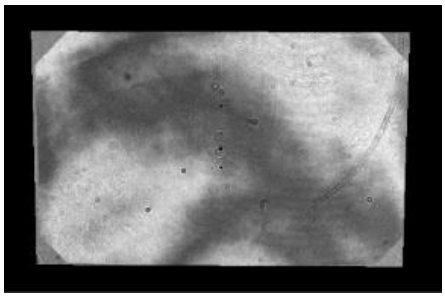

Surface Form Error	
Step	Raw AlSi40 after SPDT
RMS	52.4 nm
PV	573.7

Figure 14 : Initial shape of the AlSi mirror blank before the first thermal stabilisation sequence

After the cryogenic thermal stabilization cycles, we clearly observe a large plastic deformations of the mirror blank surface, with very high spatial frequencies. These are resulting from dislocations and stress relief between material grains. Due to high spatial frequencies, the bumpy aspect of the surface is visible through fine visual inspection.

Interferogram

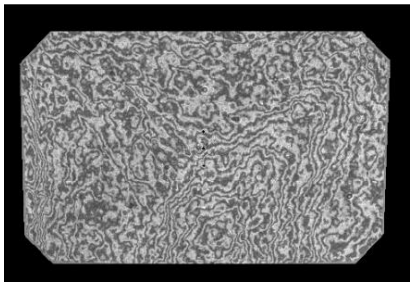

Surface Form Error	
Step	Raw AlSi40 after Thermal stabilization
RMS	998.7 nm
PV	5992.6 nm

Figure 16 : Resulting deformation of the mirror surface after the stabilization cycling

After application of the NiP layer, the mirror is submitted to a second thermal cycling treatment and then diamond turned.
Finally, an IBF run is performed for improving the SFE to 18.9 nm rms.

Surface map

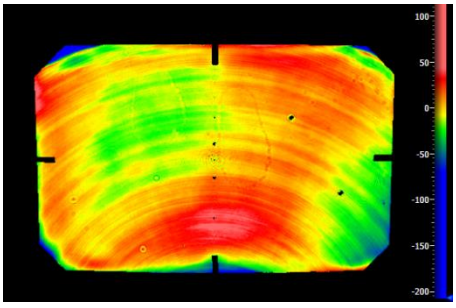

Surface Form Error	
Step	After IBF run #1
RMS	18.91 nm
PV	331.3 nm

Figure 17 : Final surface shape after a single IBF run.

After final figuring, the mirror has been submitted to 8 qualification TVAC cycling between -10 °C and 50°C. The goal of the test is to verify that the achieved stability of the mirror is sufficient to guarantee the steady performance during the mission lifetime.

After this qualification test, the mechanical surface SFE remain unchanged with a value of 18.7 nm RMS

Surface map

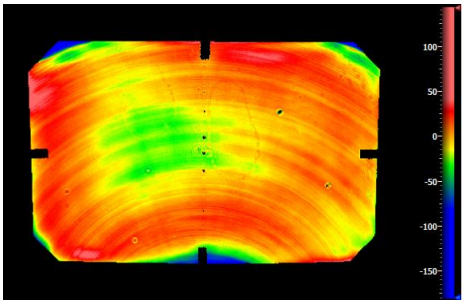

Surface Form Error	
Step	After TVAC Cycling
RMS	18.669 nm
PV	324.15 nm

Figure 18 : Surface shape after a TVAC Qualification thermal cycles.

As a conclusion we validated that the mirror is stable and there is no significant variation of the SFE value before and after TVAC qualification campaign, hence the same value before and after the test. Pixel-to-pixel subtraction only reveals small variable constraints induced by the mirror mounting to carry out the measurements.

4.2 LOW ROUGHNESS MIRROR CRYOGENIC STABILITY

The CTE of AlSi40 and NiP finely match so that it is expected that the mirror shall not experience a significant bi-metallic stress even for rather large thermal excursion. This shall be demonstrated on the LR mirror, cooled down to 200K under vacuum condition.

A dedicated setup, described in Figure 19, has been implemented for the test of the surface shape deformation under thermal vacuum.

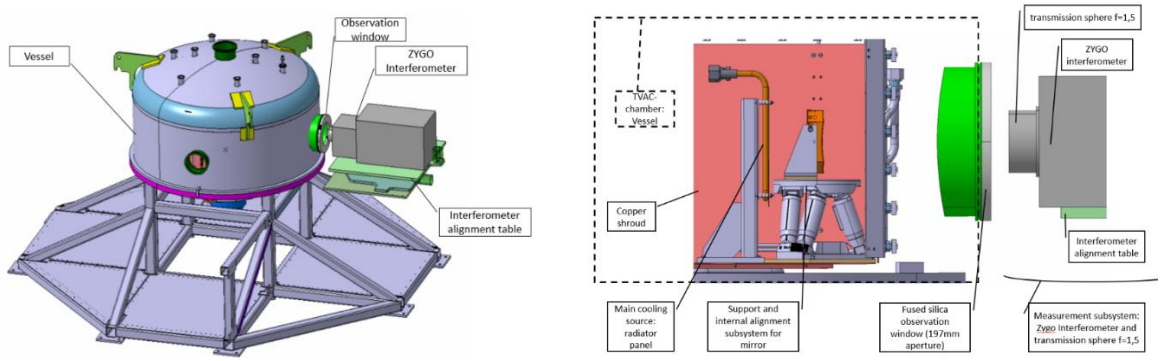

Figure 19 : Overview of the external and internal arrangement of the test vessel

The mirror is cooled down to 200K using a radiator located close to its the back face. During the test, the Rigid-body motions of the setup was corrected by a vacuum-compatible Hexapod.

The interferometer is located outside the chamber and equipped with a F/1.5 reference sphere. The beam that passes through the viewport is highly convergent. Zemax model of the setup shows that the beam will be affected

by a significant spherical aberration (~ 1 wave) and Coma (depending of the parallelism of the faces and chief ray incidence angle). Nevertheless, these aberrations produced by the viewport are expected stable during the test.

The following graphs report the Mirror temperature during the test. The flat regions of the temperature curve are corresponding to interferometric measurement periods.

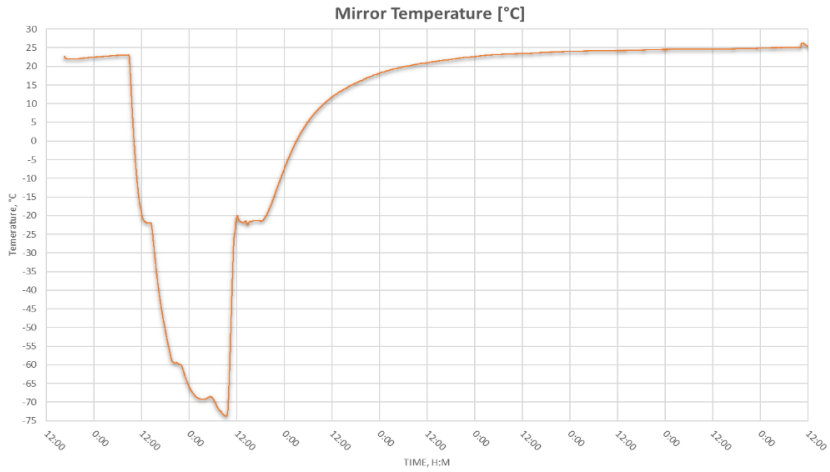

Figure 20 : LR Mirror temperature tracking during the TVAC test (in °C).

The Figure 21 report the variation of each relevant Zernike coefficients (tip, tilt and focus are not considered as they results from homothety and Rigid Body motion of the mirror). The residual RMS (orange curve) are representing the stability of the higher spatial frequencies over the mirror.

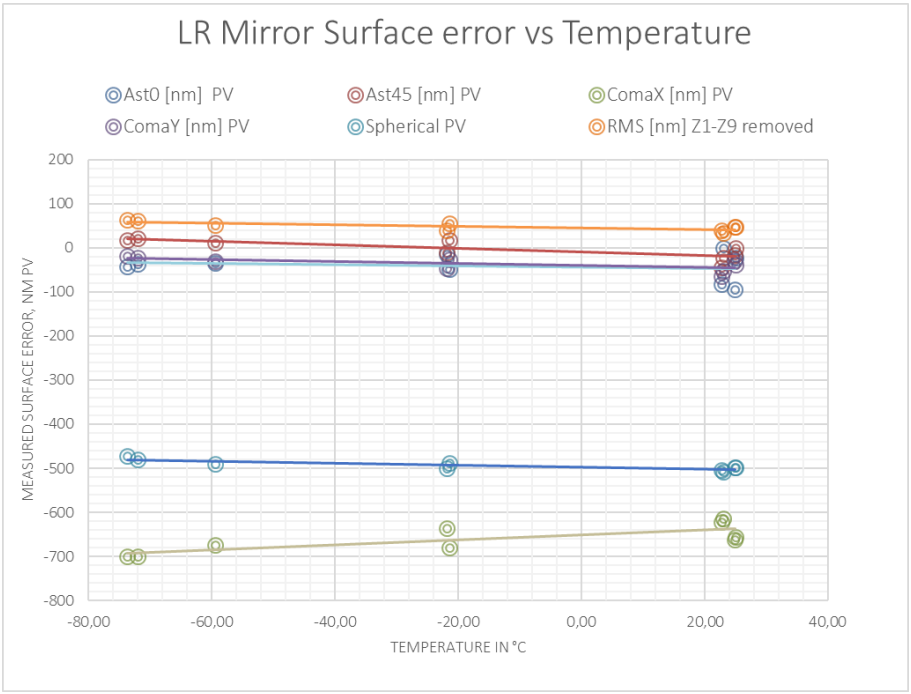

Figure 21 : Thermal Stability results for the LR mirror SFE, decomposed in Zernike fringe coefficients+ high frequencies RMS value. Best linear fit is also reported.

The stability results are summarized in the following Table 1. It recaps the RMS variation of each Zernike coefficient extrapolated over 100K. As the Zernike functions are orthogonal, the total variation of the mirror SFE (in rms) is computed through the RSS sum of each coefficients and the residual.

The results show a variation of 34 nm RMS/100K but also a residual deformation of the mirror after the test (essentially coma). This can be explained by a material stress relaxation at very low temperature. As the mirror blank itself have been submitted to cryogenic relaxation cycles before Nickle plating, a plausible origin of the observed deformation is a relaxation within the NiP layer itself or at the level of the interface between the substrate and the plating. As a mitigation, for future mirrors it is now suggested to performs the cryogenic relaxation cycles after Nickel plating rather than before.

Table 1 : SFE variation over 100K as measured on each Zernike coefficient and residual higher frequencies.

	Variation RMS	
Coefficient	RMS Variation over 100K	Before/after test
Ast0	5.3 nm	4.8 nm
Ast45	16.7 nm	11.5 nm
ComaX	19.8 nm	13.8 nm
ComaY	8.1 nm	12.8 nm
Spherical	10.2 nm	2.3 nm
Residual RMS Z1-Z9 removed	18.6 nm	7.1 nm
Total	**34.8 nm**	**23.7 nm**

We finally conclude that the deformation of the LR mirror in cryogenic temperature (200K) is not negligible, in the order of magnitude of $\lambda/20$ rms SFE. Nevertheless, provided that it is correctly taken into account in the error budget, this value may be acceptable in a certain number of applications. In particular, cryogenic temperature is usually required for Infrared application where surface quality requirement is typically less stringent. The objective of < 10 nm RMS variation, expected for UV-Visible applications, can only be achieved on a thermal excursion of about 30 K, which is a reasonable limit for many instruments.

5. CONCLUSION

Through this project, AMOS and ESA aimed to assess and optimize the complete design and manufacturing process for lightweighted and highly aspherical AlSi mirrors. **The study paves the way for lower cost instruments, produced in small to medium series with production schedule secured by full deterministic convergence of the figuring and metrology approaches.** A broad review of state-of-the-art covering material, figuring and metrology methods has been carried out and presented, before selection of the appropriate workflow.

A simplified analytic approach for the definition of lightweighting geometries have been formulated and validated through Finite Element Analysis.

The manufacturing and polishing of the mirrors have been reported in this document. The most noticeable result achieved concerns the Low Roughness mirror. **The sequential implementation of Single Point Diamond turning, soft-post polishing and Ion-Beam Figuring** allowed us to achieve a specified residual wavefront error lower than 10 nm rms (<5 nm rms SFE) over a majority of 60 mm diameter sub-pupils in a **perfectly deterministic way with a convergency rate of 60% to 70%.** Two single IBF runs, each of them less than 12 hours, were sufficient for achieving the figuring of the mirror. A performance as good, or even better, was reiterated on the Spare LW

mirror since a single IBF run, with **an evaluated convergency close to 90%**, successfully bring the mirror in compliance with the project requirement.

The use of Interferometric measurement, with **Computer Generated Holograms as nulling element, still remains in our view the utmost method for Highly aspherical or freeform surface metrology**, in the context of deterministic production of highly accurate recurrent mirrors. The cost associated to this element is rapidly amortized by the excellent reproducibility and reliability of the measure that translate in time saving and guarantee of performance. Nevertheless, for less demanding optics, for single part production or when lead time is not compatible with the definition and procurement of a CGH, **alternative methods start to challenge the absolute necessity of nulling interferometry.** We explored in the project the potential of a **phase-shifting deflectometer** that can be directly integrated in the SPDT lathe. The calibration and reliability of this device shall be improved but a sufficient resolution, especially efficient for waviness errors, has been demonstrated.

Finally, **a major achievement of the project is related to the thermal stability of the Nickel-plated Aluminium Silicon alloy**. We have applied and validated a cryogenic treatment for removing residual stress and improve the long-term stability of the produced mirrors. This stability has been successfully demonstrated through a qualification TVAC cycling test on the spare LW mirror. The stabilisation also brings a significant improvement for the IBF process. In particular we report a much lower convergence rate for the figuring of the first LW mirror that has not be submitted to the cryo-treatment.

The performance of a 100x100 mm² AlSi40 mirrors in cryogenic conditions have been evaluated through a monitoring test of the Surface Error under TVAC conditions. The test concludes to a moderate, but not negligible deformation, of the optical surface with a residual hysteresis that can be attributed to a further relaxation of stress between the NiP layer and the substrate. **We recommend additional developments before proposing the use of AlSi40 in challenging cryogenic applications, but the athermal behaviour is confirmed for a thermal range of +/- 30°C around ambient, which is a typical excursion for most of UV/VIS/NIR/SWIR earth observation mission.**